Dynamic network centrality summarizes learning in the human brain

Alexander V. Mantzaris*

Department of Mathematics and Statistics, University of Strathclyde, Glasgow, UK

Danielle S. Bassett

Department of Physics, University of California, Santa Barbara, CA 93106, USA
Sage Center for the Study of the Mind, University of California, Santa Barbara, CA 93106, USA

Nicholas F. Wymbs

Department of Psychological and Brain Sciences, University of California, Santa Barbara, CA 93106, USA

Ernesto Estrada

Department of Mathematics and Statistics, University of Strathclyde, Glasgow, UK

Mason A. Porter

Oxford Centre for Industrial and Applied Mathematics, Mathematical Institute, University of Oxford, Oxford OX1 3LB, UK
CABDyN Complexity Centre, University of Oxford, Oxford OX1 1HP, UK

Peter J. Mucha

Department of Mathematics, Carolina Center for Interdisciplinary Applied Mathematics, University of North Carolina, Chapel Hill, NC 27599-3250, USA
Institute for Advanced Materials, Nanoscience and Technology, University of North Carolina, Chapel Hill, NC 27599-3216, USA

Scott T. Grafton

Sage Center for the Study of the Mind, University of California, Santa Barbara, CA 93106, USA

and

Desmond J. Higham

Department of Mathematics and Statistics, University of Strathclyde, Glasgow, UK
*Corresponding author: alexander.mantzaris@strath.ac.uk

Edited by: P. Csermely

We study functional activity in the human brain using functional magnetic resonance imaging and recently developed tools from network science. The data arise from the performance of a simple behavioural motor learning task. Unsupervised clustering of subjects with respect to similarity of network activity measured over 3 days of practice produces significant evidence of 'learning', in the sense that subjects typically move between clusters (of subjects whose dynamics are similar) as time progresses.

However, the high dimensionality and time-dependent nature of the data makes it difficult to explain which brain regions are driving this distinction. Using network centrality measures that respect the arrow of time, we express the data in an extremely compact form that characterizes the aggregate activity of each brain region in each experiment using a single coefficient, while reproducing information about learning that was discovered using the full data set. This compact summary allows key brain regions contributing to centrality to be visualized and interpreted. We thereby provide a proof of principle for the use of recently proposed dynamic centrality measures on temporal network data in neuroscience.

1. Motivation

A network-science perspective can give valuable insights into neuroscience data sets [1]. In particular, it is useful for summarizing and comparing network properties in terms of a few key features [2–4], discovering cohesive groups of cortical regions and other important patterns [5–7] and identifying important (i.e. 'central') brain regions [8,9].

Research on networks in neuroscience has focused primarily on static situations (because this allows one to use well-established tools [10]), but the rich temporal sampling produced by neurophysiological methods, including functional magnetic resonance imaging (fMRI), offers the opportunity to study network properties that vary over time. Such *dynamic* or *temporal* networks arise in many other applications, including mobile phone communication [11], interactions in online social networks [12], criminal activities [13], voting in political bodies and much more [14]. One way to study temporal networks is to develop time-dependent generalizations of classical network 'centrality' measures [10,15], which are designed to measure which nodes (or other network structures) are important in a network. Different notions of centrality correspond to different notions of what it means for a node or edge to be important.

The aim of the present paper is to test a recently proposed temporal centrality measure designed to quantify 'communicability' in dynamic networks [16], using fMRI measurements of brain activity in people as they learn a new motor skill. The work uses a known—but modern—method on previously analysed data. Its novelty lies in (a) showing for the first time that the method has value in this neuroscience setting and (b) interpreting these results. In particular, we show that the method allows us to extract highly compressed and easy-to-interpret summaries at the level of brain regions that characterize changes occurring through learning. The work also provides further evidence that time-dependent fMRI data can contain meaningful information when regarded as a time-dependent network.

The remainder of this paper is organized as follows. In Section 2, we discuss the data that we use and what we aim to achieve in our analysis. In Section 3, we review 'communicability' in dynamic networks. We present our results in Section 4 and discuss their implications in Section 5.

2. Data and aims

We study brain activity using the non-invasive neuroimaging technique of fMRI, which provides a quantitative measurement of regional changes in blood oxygen level dependent signals that are determined in part by changes of local neuronal activity [17]. Our goal in this study is to identify meaningful temporal patterns related to functional brain networks changing over a time scale of minutes to days. We therefore examine fMRI data that were acquired during a simple learning task in which 20 subjects practised short sequences of finger movements (12 movements per sequence type) over the course of 3 days [5,18]. Our data set is therefore composed of 60 experimental sessions.

We construct dynamic functional brain networks by first parcellating the brain into 112 anatomically distinct areas, which we represent as network nodes. We then partition the mean signal from each of these regions from all experimental sessions into 25 time steps of roughly 3 min duration each (corresponding to a time series of 80 units in length). Thus, the full experiment consists of 25 time steps per subject. To estimate the interactions (i.e. the edge weights) between nodes, we calculate a measure of statistical similarity between regional activity profiles. Using a wavelet transform, we extract frequency-specific activity from each time series in the range 0.06–0.12 Hz. For each subject s, each experimental day d, each time step t and each pair of regions i and j, we define the weight of an edge connecting regions i and j as the coherence between the wavelet coefficient time series in each region (other measures of similarity are also possible [19]), and these weights form the elements of a weighted temporal network $\mathbf{A}$ with components $[\mathbf{A}_{s,d}^{[t]}]_{i,j}$, where $s \in \{1, \ldots, 20\}$, $d \in \{1, 2, 3\}$ and $t \in \{1, \ldots, 25\}$.

We used a statistical correction (the false discovery rate) to threshold all connections for which we were not confident that the coherence value was significantly greater than that expected between random variables, and we then binarized the data. Specifically, $[\mathbf{A}_{s,d}^{[t]}]_{i,j} = 1$ if and only if the fMRI time series from regions i and j demonstrates statistically significant temporal coherence for subject s on day d at the tth time step of the experiment. We set all other $[\mathbf{A}_{s,d}^{[t]}]_{i,j}$ to 0. We kept approximately 9% of the measured connections (i.e. the edges) as statistically significant. We can therefore view each experiment as a time-ordered sequence of 25 binary, symmetric adjacency matrices of dimension 112×112. We also note that each diagonal entry $[\mathbf{A}_{s,d}^{[t]}]_{i,i} = 0$.

In a previous examination of these data, we used time-dependent community detection [20] to identify statistically significant temporal evolution of network organization over time [5]. We found that network 'flexibility', measured in terms of the time-varying allegiance of nodes to communities, in one experimental session predicted the relative amount of learning demonstrated in a future session. Our goal in the present work is to use a complementary approach, based on a recently proposed notion of temporal network centrality that respects the arrow of time [16], to examine the data from a different perspective. Methods to study temporal networks are being developed rapidly, and they need testbed examples. It is therefore crucial to apply multiple viable approaches to the same data and evaluate the different insights and perspectives that they offer. Very recent work has examined static centrality measures in functional brain networks [21], and our work generalizes such perspectives to time-dependent situations.

3. Dynamic communicability

Network centrality diagnostics are designed to measure which nodes (or other network structures) are important [10,15], and many of them can be motivated by considering how information flows around a network [22]. In such a perspective, central nodes are those that can use a network's connectivity structure to distribute or collect information effectively. In a time-dependent network, in which connections can appear and disappear, it is important to consider routes through the network that respect the arrow of time. For example, suppose that nodes a and b are connected today via an undirected edge and that nodes b and c are connected tomorrow via an undirected edge. The route $a \mapsto b \mapsto c$ can thus be traversed over the course of the 2 days. However, unless there are other edges, the reverse route from c to a cannot be taken, as the arrow of time introduces an asymmetry in the information flow [14].

Reference [16] quantified the ability of a node i to send information to node j across a time-dependent network by summing over all *dynamic walks* from i to j. A dynamic walk is any traversal that respects the time ordering—after reaching a node, it can continue along any edge that currently, or subsequently, involves that node. If we suppose that walks that traverse more edges are less relevant than those that traverse fewer edges, then the contribution to the sum from a walk that uses w edges is

scaled by α^w. The parameter $\alpha \in (0, 1)$ governs the extent to which we downweight a walk based on the number of edges that compose it. This methodology was introduced by Katz [23] for static, unweighted, undirected networks. (Also see the interpretation in [24].) Katz noted that α can be interpreted as the independent probability that information successfully traverses an edge. Importantly, because we binarize the data, we retain a dynamic analogue of this interpretation in the networks that we study in the present paper.

The aforementioned summary over dynamic walks quantifies how effectively node i can communicate with node j and is computed readily as the (i, j) element in a product of matrix resolvents:

$$\mathcal{P}_{s,d} := (I - \alpha\mathbf{A}_{s,d}^{[1]})^{-1}(I - \alpha\mathbf{A}_{s,d}^{[2]})^{-1} \cdots (I - \alpha\mathbf{A}_{s,d}^{[25]})^{-1}. \tag{1}$$

To explain further, we first note that resolvents can be expanded in power series:

$$(I - \alpha A)^{-1} = I + \alpha A + \alpha^2 A^2 + \cdots.$$

It then follows that the right-hand side of (1) combines all possible time-ordered matrix products (appropriately scaled). For example, we obtain terms such as the following:

- $\alpha^2\mathbf{A}_{s,d}^{[1]}\mathbf{A}_{s,d}^{[2]}$, whose (i, j) element gives a scaled count of the number of dynamic walks that involve one edge at time point $t = 1$ and one edge at time point $t = 2$ and

- $\alpha^3\mathbf{A}_{s,d}^{[2]}\mathbf{A}_{s,d}^{[4]}\mathbf{A}_{s,d}^{[4]}$, whose (i, j) element gives a scaled count of the number of dynamic walks that involve one edge at time point $t = 2$ and two edges at time point $t = 4$.

In practice, we use a normalized version,

$$\mathcal{Q}_{s,d} := \frac{\mathcal{P}_{s,d}}{\|\mathcal{P}_{s,d}\|_2}, \tag{2}$$

where $\|\cdot\|_2$ denotes the Euclidean norm, in order to avoid underflow and overflow. The matrix inverses in (1) exist as long as $\alpha < \alpha^\star$, where $\alpha^\star$ is the reciprocal of the maximum eigenvalue (in modulus) over all of the individual adjacency matrices. In this work, we use the value $\alpha = 0.9\alpha^\star$. As discussed in Grindrod *et al.* [16] and Mantzaris & Higham [25], averaging the connectivity information over time and computing the Katz centrality for this static summary (thereby ignoring the time ordering) can produce significantly different results. Accordingly, it is important to use a method that respects the time-dependent nature of the problem.

The matrix entries $\{[\mathcal{Q}_{s,d}]_{nj}\}_{j=1}^{112}$ quantify the ability of node n to disseminate information to each node in a network. One can sum over the elements in the nth row to compute an aggregate *broadcast strength* $\mathbf{b}(n)$ for node n. Similarly, by summing over the elements in the nth column of $[\mathcal{Q}_{s,d}]$, we quantify the ability of node n to receive information using the *receive strength* $\mathbf{r}(n)$. This yields the broadcast centrality

$$\mathbf{b}(n)_{s,d} := \sum_{j=1}^{112}(\mathcal{Q}_{s,d})_{nj}, \tag{3}$$

and receive centrality

$$\mathbf{r}(n)_{s,d} := \sum_{i=1}^{112}(\mathcal{Q}_{s,d})_{in}, \tag{4}$$

from Grindrod *et al.* [16].

In the next section, we demonstrate that (a) the fMRI data provide evidence of learning, in the sense that subjects typically move between different clusters (of subjects based on similar brain activity patterns), based on these centrality values, as time progresses and (b) that (time-respecting) dynamic communicability captures the same effect in a low-dimensional summary that is amenable to visualization and interpretation.

4. Results

We seek brain signatures that reflect learning-related changes as subjects acquire a new motor skill and improve in performance. We do this by treating each experimental session as a data point and performing unsupervised k-means clustering [26] to separate the experiments into two groups. We then view the clusters in terms of their subject/day identifications (IDs) to determine whether the two clusters represent different stages of learning.

In Table 1 (full temporal data), we show the clustering that we obtain when we represent each experiment using its full set of connectivity data—i.e. when we stack the matrices $\{\mathbf{A}_{s,d}^{[t]}\}_{t=1}^{25}$ column by column into a single vector of dimension $112 \times 112 \times 25 = 313,600$. We hypothesize that cluster 2 might represent a higher level of 'ability' or 'experience' and hence that moving from cluster 1 to cluster 2 represents the result of learning. To be more concrete, we regard the data clustering as a 'success' for subject s if the cluster label does not decrease either between Day 1 and Day 2 or between Day 2 and Day 3. In other words, a subject is successful if he/she does not exhibit a decrease in learning-related changes in brain function. For example, Subject 1 in Table 1 (full temporal data) has the sequence $1, 1, 2$ and Subject 3 has the sequence $1, 2, 2$. We regard both subjects as successful. Subject 9, who has the sequence $2, 2, 2$, is also successful. However, Subject 5 has the sequence $1, 2, 1$, and we therefore regard this subject as not successful. In total, the 20 subjects exhibit 17 successes and 3 failures (Subjects 5, 8 and 20). Using a permutation test, where we redistribute cluster labels A and B uniformly at random across experiments and map the labels A and B to the labels 1 and 2 in a way that minimizes the number of failures, we find that the achievement of 17 or more successes has a p-value of ≈ 0.0025. For this example (as well as all of our other k-means computations), we note that multiple runs with different starting values yield very similar results.

In Table 1 (dynamic communicability matrix), we show the corresponding results that we obtain when we summarize each experiment (of 25 time points) using its dynamic communicability matrix (2), which we stack column by column into a vector of dimension $112 \times 112 = 12,544$. We again observe 17 successful subjects and 3 failures (Subjects 5, 11 and 17).

We also apply the same clustering approach with each experiment collapsed to a vector of either broadcast (3) or receive (4) centralities, where we recall that each component of either vector represents a single brain region. Using either of these vectors, which have a dimension of only 112, we find identical results as with the $12,544$-dimensional description.

The aforementioned results suggest (i) that there is evidence that the fMRI data have captured a learning effect and (ii) that the evidence remains intact even when we vastly reduce the dimension of the data by using only broadcast or receive centrality measures, which have a natural interpretation in terms of quantifying the ability of a brain region to distribute or collect information.

Because the broadcast and receive centralities relate directly to individual brain regions, we follow up on the results in Table 1 and study how these centralities vary over time. We find that broadcast and receive centralities both decrease appreciably over the 3 days of the experiment, suggesting their potential sensitivity to learning (see Fig. 1(a)). In addition to their temporal dependence, these two types of centrality vary over individuals in the experiment (see the error bars in Fig. 1(a)) and over brain

TABLE 1 *Results of unsupervised k-means clustering into two groups, displayed by subject and by day, using the full temporal data* (*which has dimension* 313,600) *and by summarizing each experiment in terms of the dynamic communicability matrix* (2) (*which has dimension* $112 \times 112 = 12,544$). *We also obtain the same results using a vector of either the broadcast centralities* (3) *or the receive centralities* (4). *Each of these descriptions has a dimension of only* 112

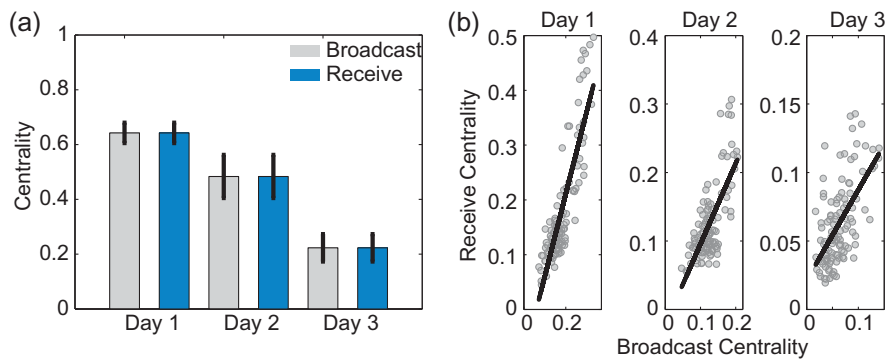| Subject ID	1	2	3	4	5	6	7	8	9	10	11	12	13	14	15	16	17	18	19	20
Full temporal data																				
Day 1	1	1	1	1	1	1	1	1	2	2	2	1	1	2	1	1	2	1	1	2
Day 2	1	1	2	1	2	1	1	2	2	2	2	1	2	2	2	1	2	2	1	1
Day 3	2	2	2	2	1	2	2	1	2	2	2	2	2	2	2	2	2	2	2	1
Dynamic communicability matrix																				
Day 1	1	1	1	1	1	1	1	1	1	1	1	1	1	1	1	1	1	1	1	1
Day 2	1	1	2	1	2	1	1	1	2	1	2	1	1	1	2	1	2	1	1	1
Day 3	2	1	2	2	1	2	2	1	2	2	1	2	2	1	2	2	1	2	2	1

FIG. 1. Broadcast and receive centralities change with task learning. (a) Bar graph showing broadcast (light) and receive (dark) centralities averaged over brain regions for Days 1, 2 and 3 of the experiment. Error bars indicate standard deviations of the mean over subjects. (b) Scatter plots showing the Pearson correlations between broadcast and receive centralities for Day 1 (correlation coefficient $r \approx 0.86$; *p*-value $\approx 2.4 \times 10^{-35}$), Day 2 ($r \approx 0.71$; $p \approx 6.6 \times 10^{-19}$) and Day 3 ($r \approx 0.60$; $p \approx 1.8 \times 10^{-12}$) of the experiment.

regions (see Fig. 1(a)). We also find that broadcast and receive centralities are strongly correlated with one another over brain regions for all 3 days of the experiment (see Fig. 1(b)).

From the above results, it is unclear whether the broadcast and receive centralities for each brain region decrease similarly over days or whether the values for some brain regions decrease more than those for others. We therefore test whether any brain region has a change in its centrality values between Day 1 and Day 3 that is more than what is expected given the aggregate decrease shown in Fig. 1(a). To do this, we normalize the broadcast and receive centrality vectors from the 60 communicability matrices separately. For each region, we then test whether the normalized centrality values differ significantly in Day 1 versus Day 3 using a permutation test in which we permuted the Day 1 and Day 3 labels uniformly at random. We find that no brain region demonstrates a significant decrease in either normalized
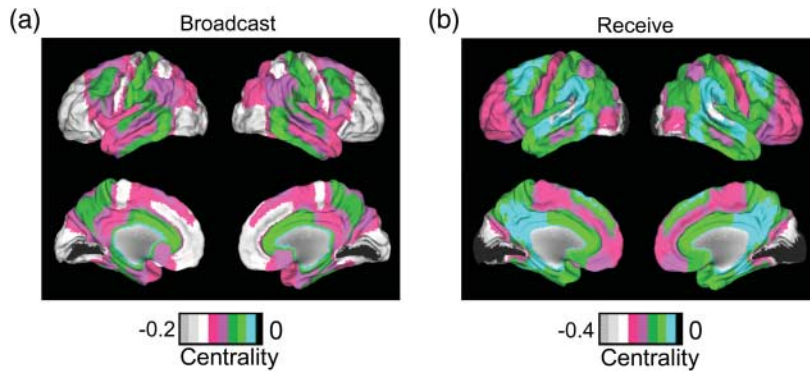
FIG. 2. Anatomical distribution of decrease over time (Day 3 minus Day 1) in broadcast and receive centralities. Broadcast (a) and receive (b) centralities with normalized centrality vectors over subjects.

broadcast centrality or normalized receive centrality from Day 1 to Day 3 ($p > 0.01$; uncorrected for multiple comparisons).

In light of the result that brain regions do not differ significantly from each other in the amount of centrality change with learning, one can study the change in anatomical distribution of centrality values by normalizing each experiment's centrality values, aggregating the normalized regional components from all the 60 experiments and then viewing the difference in the aggregations over regions (see Fig. 2). We find that there is a decrease in aggregate centrality over time for all regions, and that the decreases in dynamic centrality values are greatest in bilateral precentral gyri (primary motor cortex), medial segment of the superior frontal gyrus (supplementary motor area), superior parietal lobule and medial occipital cortices. This constellation of regions is a core sensorimotor system for controlling a broad range of visually guided actions [27], including the motor task of this study. Of particular note, two of these areas—the primary motor cortex and SMA—are consistently observed to demonstrate changes in local activity [28–30] as well as changes in correlated activity during sequence learning [31].

5. Discussion

Our results indicate a striking decrease in broadcast and receive centrality as subjects improve with practice. Learning-related changes in both activity and connectivity could underlie these network signatures. For example, theoretical work indicates an increase in neural efficiency with learning [32]. In this view, greater skill at applying an initial task-related strategy leads to a temporal increase in the efficiency of neural processing, which can manifest as an aggregate decrease in measurements of brain activity [33]. It is also possible that decreasing dynamic network centrality reflects a form of adaptation, leading to a more efficient configuration in terms of the amount of connectivity required to sustain the motor task. Alternatively, the change in communicability might alter the way in which the brain executes the motor task by using a more decentralized (but clustered) organization.

The development of new tools for investigating time-dependent networks would be extremely useful for distinguishing these various accounts of brain network modulation during learning. Indeed, it has been suggested that an understanding of such changes and their relationship to neural efficiency will require a more careful examination of functional connectivity patterns [34], which are thought to be better indications of neuronal communication than activity patterns alone [35]. The present paper highlights the potentially important effect of temporal dynamics in the consideration of neural efficiency,

and recent methodological advances for the investigation of time-dependent networks [14] now make it possible to pursue such efforts. We demonstrate decreases in functional connectivity patterns with task practice in early motor learning, suggesting that the brain might require less communication between distributed functional networks as skills become more automatic.

The ideas that we have employed in this study have important potential applications not only in the setting of fMRI experiments but also in the examination of functional neuroscience data using other experimental modes. Interest in studying whole-brain functional connectivity patterns in a network framework is growing steadily [1], in part because network science includes a large set of diagnostics that are built to directly examine system connectivity and can be used to characterize the brain's structural organization. However, a study of the true dynamic nature of the brain requires the use of dynamic network diagnostics, the development of which is still in its early stages [14]. We have demonstrated in this paper that broadcast and receive centralities are useful diagnostics for the study of temporal brain networks, and they have the additional advantage of respecting the arrow of time. We expect such dynamic centrality measures to be similarly insightful in a wide variety of systems.

References

1. Bullmore, E. & Sporns, O. (2009) Complex brain networks: graph theoretical analysis of structural and functional systems. *Nat. Rev. Neurosci.*, **10**, 186–198.
2. Crofts, J. J. & Higham, D. J. (2009) A weighted communicability measure applied to complex brain networks. *J. R. Soc. Interface*, **33**, 411–414.
3. Deuker, L., Bullmore, E. T., Smith, M., Christensen, S., Nathan, P. J., Rockstroh, B. & Bassett, D. S. (2009) Reproducibility of graph metrics of human brain functional networks. *NeuroImage*, **47**, 1460–1468.
4. Rubinov, M. & Sporns, O. (2010) Complex network measures of brain connectivity: uses and interpretations. *NeuroImage*, **52**, 1059–1069.
5. Bassett, D. S., Wymbs, N. F., Porter, M. A., Mucha, P. J., Carlson, J. M. & Grafton, S. T. (2011) Dynamic reconfiguration of human brain networks during learning. *Proc. Natl Acad. Sci.*, **18**, 7641–7646.
6. Crofts, J. J. & Higham, D. J. (2011) Googling the brain: discovering hierarchical and asymmetric network structures, with applications in neuroscience. *Internet Math.*, **7**, 1–22.
7. Johansen-Berg, H., Behrens, T. E. J., Robson, M. D., Drobnjak, I., Rushworth, M. F. S., Brady, J. M., Smith, S. M., Higham, D. J. & Matthews, P. M. (2004) Changes in connectivity profiles define functionally-distinct regions in human medial frontal cortex. *Proc. Natl Acad. Sci.*, **101**, 13335–13340.

8. SPORNS, O., TONONI, G. & KÖTTER, R. (2005) The human connectome: a structural description of the human brain. *PLoS Comput. Biol.*, **1**, 245–251.

9. ZAWADZKI, K., FEENDERS, C., VIANA, M. P., KAISER, M. & COSTA, L. D.F. (2012) Morphological homogeneity of neurons: Searching for outlier neuronal cells. *Neuroinformatics*, **10**, 379.

10. NEWMAN, M. E. J. (2010) *Networks: An Introduction*. Oxford: Oxford University Press.

11. ONNELA, J.-P., SARAMÄKI, J., HYVÖNEN, J., SZABÓ, G., LAZER, D., KASKI, K., KERTÉSZ, J. & BARABÁSI, A. L. (2007) Structure and tie strengths in mobile communication networks. *Proc. Natl Acad. Sci.*, **104**, 7332–7336.

12. SZELL, M., LAMBIOTTE, R. & THURNER, S. (2010) Trade, conflict and sentiments: multi-relational organization of large-scale social networks. *Proc. Natl Acad. Sci.*, **107**, 13636–13641.

13. STOMAKHIN, A., SHORT, M. B. & BERTOZZI, A. L. (2011) Reconstruction of missing data in social networks based on temporal patterns of interactions. *Inverse Probl.*, **27**, 115013.

14. HOLME, P. & SARAMÄKI, J. (2012) Temporal networks. *Phys. Rep.*, **519**, 97–125.

15. WASSERMAN, S. & FAUST, K. (1994) *Social Network Analysis: Methods and Applications*. Cambridge: Cambridge University Press.

16. GRINDROD, P., HIGHAM, D. J., PARSONS, M. C. & ESTRADA, E. (2011) Communicability across evolving networks. *Phys. Rev. E*, **83**, 046120.

17. LOGOTHETIS, N., PAULS, J., AUGATH, M., TRINATH, T. & OELTERMANN, A. (2001) Neurophysiological investigation of the basis of the fMRI signal. *Nature*, **412**, 150–157.

18. WYMBS, N. F., BASSETT, D. S., MUCHA, P. J., PORTER, M. A. & GRAFTON, S. T. (2012) Differential recruitment of the sensorimotor putamen and frontoparietal cortex during motor chunking in humans. *Neuron*, **74**, 936–946.

19. SMITH, S. M., MILLER, K. L., WEBSTER, M., SALIMI-KHORSHIDI, G., BECKMANN, C. F., NICHOLS, T. E., RAMSEY, J. D. & WOOLRICH, M. W. (2011) Network modelling methods for fMRI. *NeuroImage*, **54**, 875–891.

20. MUCHA, P. J., RICHARDSON, T., MACON, K., PORTER, M. A. & ONNELA, J.-P. (2010) Community structure in time-dependent, multiscale, and multiplex networks. *Science*, **328**, 876–878.

21. KUHNERT, M.-T., GEIER, C., ELGER, C. E. & LEHNERTZ, K. (2012) Identifying important nodes in weighted functional brain networks: a comparison of different centrality approaches. *Chaos*, **22**, 023142.

22. ESTRADA, E. (2011) *The Structure of Complex Networks*. Oxford: Oxford University Press.

23. KATZ, L. (1953) A new index derived from sociometric data analysis. *Psychometrika*, **18**, 39–43.

24. BONACICH, P. (1987) Power and centrality: a family of measures. *Am. J. Sociol.*, **92**, 1170–1182.

25. MANTZARIS, A. V. & HIGHAM, D. J. (2012) A model for dynamic communicators. *Eur. J. Appl. Math.*, **23**, 659–668.

26. GAN, G., MA, C. & WU, J. (2007) *Data Clustering: Theory, Algorithms, and Applications*. Philadelphia, PA: Society for Industrial and Applied Mathematics.

27. BERNIER, P. M. & GRAFTON, S. T. (2010) Human posterior parietal cortex flexibly determines reference frames for reaching based on sensory context. *Neuron*, **68**, 776–788.

28. BISCHOFF-GRETHE, A., GOEDERT, K. M., WILLINGHAM, D. T. & GRAFTON, S. T. (2004) Neural substrates of response-based sequence learning using fMRI. *J. Cogn. Neurosci.*, **16**, 127–138.

29. GRAFTON, S., HAZELTINE, E. & IVRY, R. (1995) Functional mapping of sequence learning in normal humans. *J. Cogn. Neurosci.*, **7**, 497–510.

30. HAZELTINE, S. T., GRAFTON, E. & IVRY, R. (1995) Attention and stimulus characteristics determine the locus of motor-sequence encoding. A PET study. *Brain J. Neurol.*, **120**, 123–140.

31. SUN, F. T., MILLER, L. M., RAO, A. A. & D'ESPOSITO, M. (2007) Functional connectivity of cortical networks involved in bimanual motor sequence learning. *Cereb. Cortex*, **120**, 1227–1234.

32. GOBEL, E. W., PARRISH, T. B. & REBER, P. J. (2007) Neural correlates of skill acquisition: decreased cortical activity during a serial interception sequence learning task. *NeuroImage*, **58**, 1150–1157.

33. LANDAU, S. M. & D'ESPOSITO, M. (2006) Sequence learning in pianists and nonpianists: an fMRI study of motor expertise. *Cogn. Affect. Behav. Neurosci.*, **6**, 246–259.

34. KELLY, A. M. & GARAVAN, H. (2005) Human functional neuroimaging of brain changes associated with practice. *Cereb. Cortex*, **15**, 1089–1102.

35. SUN, F. T., MILLER, L. M. & D'ESPOSITO, M. (2006) Measuring inter-regional functional connectivity using coherence and partial coherence analyses of fMRI data. *NeuroImage*, **21**, 647–658.